LAWRENCE
LIVERMORE
NATIONAL
LABORATORY

LLNL-JRNL-404948

Titanium-Dioxide Nano-Fiber-Cotton Targets for Efficient Multi-keV X-Ray Generation

M. Tanabe, H. Nishimura, S. Fujioka, K. Nagai, N. Yamamoto, Z.-Z. Gu, C. Pan, F. Girard, M. Primout, B. Villette, D. Brebion, K. B. Fournier, A. Fujishima, K. Mima

June 25, 2008

Applied Physics Letters

Disclaimer

Titanium-dioxide nano-fiber-cotton targets for efficient multi-keV x-ray generation

Minoru Tanabe,[1,*] Hiroaki Nishimura,[1] Shinsuke Fujioka,[1] Keiji Nagai,[1] Norimasa Yamamoto,[1] Zhong-Ze Gu,[2] Cao Pan,[2] Frederic Girard,[3] Michel Primout,[3] Bruno Villette,[3] Didier Brebion,[3] Kevin B. Fournier,[4] Akira Fujishima,[5] and Kunioki Mima[1]

[1]*Institute of Laser Engineering, Osaka University, 2-6 Yamada-Oka, Suita, Osaka, 565-0871 Japan*

[2]*State Key Laboratory of Bioelectronics, Southeast University, Nanjing, Jiangsu, 210096, People's Republic of China*

[3]*Commissariat a l'Energie Atomique, DAM-Ile-de-France, Bruyeres-le-Chatel, 91297, Arpajon, Cedex, France*

[4]*Lawrence Livermore National Laboratory, P.O. Box 808, L-473, Livermore, California, 94550, USA*

[5]*Kanagawa Academy of Science and Technology, 3-2-1 Sakato, Kozu-ku, Kawasaki, 213-0012 Janpan*

Abstract

Multi-keV x-ray generation from low-density (27±7 mg/cc) nano-fiber-cotton targets composed of titanium-dioxide has been investigated. The cotton targets were heated volumetrically and supersonically to a peak electron temperature of 2.3 keV, which is optimal to yield Ti *K*-shell x rays. Considerable enhancement of conversion efficiency ($3.7 \pm 0.5\%$) from incident laser energy into Ti *K*-shell x rays (4-6 keV band) was attained in comparison with that ($1.4 \pm 0.9\%$) for a planar Ti-foil target.

PACS numbers: 52.38.Ph, 52.50.Jm, 52.70.La

Efficient multi-keV x-ray sources are useful for probing dense matter in the fields of high-energy-density physics and inertial-confinement-fusion experiments [1]. High conversion efficiency (CE), high photon energy, and uniformity of the x-ray sources are required in these applications. Multi-keV x rays are emitted from highly ionized high-Z ions [2–7] or from inner-shell-ionized high-Z atoms ionized by fast electron impacts [8].

For highly ionized plasmas, multi-keV x-ray generation has been investigated with various kinds of targets, including solids [2–4], gases in an enclosure [5, 6], and high-Z doped aerogels [7]. In the case of the solid targets, CE shows a strong logarithmic decrease with increasing photon energy [9]. In addition, the one-dimensional radiation-hydrodynamic code (ILESTA-1D [10]) predicts that for solid targets the thickness of an optimal multi-keV x-ray generating region is about 100 μm because of steep gradients of density and temperature. In the case of low-density high-Z targets, laser energy is mostly absorbed by inverse bremsstrahlung; the targets are heated supersonically and volumetrically without hydrodynamic expansion [11, 12] creating a large x-ray emitting region. Thus the heating mechanisms of the target are one key to generating multi-keV x rays efficiently [5, 7, 13, 14].

In this work, we use a low-density, high-Z doped target composed of titanium-dioxide (TiO_2) nano-fiber-cotton [15] to generate 4.7 keV x rays. The following will be discussed in this paper: temporal evolution of electron temperature, supersonic heat-wave propagation into the target, and absolute Ti K-shell x-ray yields from the targets.

The TiO_2 nano-fiber-cotton targets are fabricated with the electrospinning method [15, 16]. This method enables us to fabricate low-density materials containing various high-Z atoms that exist as a metal-oxide. The diameter of each fiber is less than 100 nm and its typical length is several 10's of μm. Mass density of the nano-fiber-cotton used in this study was 27 ± 7 mg/cc. Assuming full ionization of the target, electron density was equal of 0.8 ± 0.2 times the critical density for 0.351 μm laser light. A small block of the nano-fiber-cotton material was sliced into targets of 0.8 mm thickness, 1.5 mm width, and 2.5 mm height, and attached to a 50-μm-thick polystyrene film.

Experiments were performed on the GEKKO XII laser facility in the Institute of Laser Engineering, Osaka University. Laser wavelength and pulse shape were, respectively, 0.351 μm and 1.0 ns full width at half maximum Gaussian. Eight beams of the GEKKO XII laser were bundled into a cone with a half angle of 9.4 degrees and were focused at 100 μm in front of the target surface. The laser intensity on the target surface was approximately 1×10^{15} W/cm^2.

Four kinds of x-ray diagnostics were used simultaneously to measure Ti K-shell emission from the targets as shown in Fig. 1. A photometrically calibrated x-ray diode array (XRDs) was installed on the laser-illumination side to measure CE into x rays in the range of 4-6 keV. Uncertainty of the measured CE is $\pm 15\%$ for the unfolded results from the diodes. Time-resolved x-ray spectra from 4.8 to 5.7 keV were observed from the direction perpendicular to the incident laser axis by means of a flat rubidium acid phthalate crystal spectrometer coupled to x-ray streak camera, the so-called x-ray streaked spectrograph (XSS). Temporal resolution was 20 ps and spectral resolution $E/\Delta E$ (E : photon energy) was 200. To restrict the observation region and also to achieve high spectral resolution, a 100-μm-width slit was set in the line-of-sight of the XSS and at 1.5 mm distance from the target surface. The substrate of the slit was a 50-μm-thick tantalum foil. The observation region was chosen to be 50-150 μm behind the target surface. A gated x-ray framing camera (XFC) was installed to observe heat-wave propagation into the target perpendicular to the incident laser axis. Spatial resolution of the XFC was 23 μm and exposure time was 80 ps. A K-edge absorption filter of 5-μm-thick titanium foil was set in the XFC to detect photon energy from 4.7 keV to 4.9 keV. To observe trajectory of the heat-wave front, an x-ray streak camera (XSC) was installed. The XSC was set at 25 degrees with respect to the XFC. A K-edge absorption filter of 10-μm-thick titanium foil was used. Temporal resolution of the XSC was 52 ps and the spatial resolution was 23 μm.

Figure 2 shows a measured Ti K-shell x-ray spectrum (solid line) from the nano-fiber-cotton at the time of the highest electron temperature. The Ti-Lyα, Heβ resonance, and lithium-like satellite lines are identified. The Lyα line is partly overlapped with the dielectronic satellite transitions (He-like satellites) due to the limited spectral resolution of the XSS.

An atomic kinetics model, the FLYCHK code [17], was used to derive electron temperatures from the measured spectra. The line intensity ratio of the resonance transition (Lyα) to a dielectric satellite transitions (He-like satellites) as well as the ratio of the Lyα line to Heβ line were adopted for this analysis. The electron density was assumed to be 8.8×10^{21} cm^{-3}. Spectra calculated by the FLYCHK code were convolved with the instrumental spectral resolution of the XSS. The synthetic spectra for electron temperatures of 1.8 keV, 2.3 keV, and 2.8 keV are also presented in Fig. 2. These spectra are normalized by the Lyα line intensity. In the FLYCHK code, the dielectronic satellite transitions that are the red wing of the Heβ are not included, which is why they are absent in Fig. 2. Given that, the measured spectrum agrees quite well with the synthetic spectrum for electron temperature of 2.3 keV. Spectra measured at other times during this shot

indicate electron temperatures were in the range of 1.6 - 2.3 keV. The FLYCHK code also predicts that a plasma with an electron temperature 2.0 - 2.5 keV, and at the critical density for 0.351 μm laser light, optimally generates Ti K-shell x-ray radiation (4.0-6.0 keV). Electron temperatures inferred from our experimental spectra are in this the optimal temperature range.

Figure 3 shows two-dimensional x-ray images at different times for the 20 μm-thick Ti-foil (a)-(c) and for the TiO_2 nano-fiber-cotton target (d)-(f). The time origin was defined as 10% of x-ray emission peak obtained with the XSS. The x-ray generating region for the nano-fiber-cotton target was considerably expanded into the target along the incident laser axis; the x-ray emission region reaches approximately a millimeter in size. This result demonstrates that the target was volumetrically heated like the cases of gas and aerogel targets [5–7]. In contrast, the x-ray generating region is localized near the initial target surface for the 20-μm-thick Ti-foil. The x-ray generating region expanded into the vacuum, with a size of only 150 μm.

Trajectories of the heat-wave front were derived from the streaked images. The heat-wave front position at a particular time was defined as the $1/e$ rising edge in x-ray intensity moving along the laser axial direction. The velocity of heat-wave propagation was measured to be 5×10^7 cm/s. The sound speed was calculated adiabatically using a quotidian equation of state package [18]. The computed sound speed at the highest electron temperature of 2.3 keV is 3×10^7 cm/s. Consequently, the propagation velocity of heat-wave front is almost twice as fast as the sound speed. These results demonstrated that the TiO_2 nano-fiber-cotton targets were supersonically heated.

The CEs were defined as the ratio between the total x-ray output in the 4-6 keV band, which is measured by the XRDs, into 4π divided by the total incident laser energy. The CEs for the nano-fiber-cotton targets were $3.7\pm0.5\%$. The CE for a planar 20-μm-thick Ti-foil with a single, nanosecond laser pulse was $1.4\pm0.9\%$. The CE for the TiO_2 nano-fiber-cotton is 2.6 times higher than that for the Ti-foil. Accordingly, volumetric, supersonic heating of the targets results in the enhancement of the multi-keV x-ray conversion efficiency.

In summary, multi-keV x-ray generation using the low-density TiO_2 nano-fiber-cotton targets has been experimentally investigated. The electron temperatures derived by the time-resolved x-ray spectra were close to the optimal range for generating Ti-K shell x rays efficiently. Compared with the Ti-foil targets, an enhancement of 2.6× in the CE of laser energy was attained. The enhancement of the CE is ascribed to supersonic, volumetric heating of the nano-fiber-cotton targets. Therefore, this type of the target is suitable as an efficient multi-keV x-ray source. An interesting task to generate more highly efficient sources would involve optimization of the target structures,

composition, and density, and to clarify further the heating mechanisms of the cotton target by comparisons with simulations by the two-dimensional radiation-hydrodynamic codes [19].

The authors would like to thank Y. Yasuda and Y. Kimura for nano-fiber target fabrication. This work performed under the auspices of the U.S. Department of Energy by Lawrence Livermore National Laboratory under Contract DE-AC52-07NA27344, the Ministry of Education, Culture, Sports, Science and Technology of Japan project "Advanced Diagnostics for Burning Plasma (code 442) "Temperature and density mapping of imploded burning plasma with monochromatic x-ray imaging (code 20026005), National Basic Research Program of China (Grant No.2007CB936300), and JSPS-CAS Core-University Program in the field of "Plasma and Nuclear Fusion".

---

* Electronic address: mtanabae@ile.osaka-u.ac.jp

[1] J. Nuckolls, L. Wood, A. Thiessen, and G. B. Zimmerman, Nature (London) **239**, 139 (1972).

[2] B. Yaakobi, P. Bourke, Y. Conturie, J. Delettrez, J. M. Forsyth, R. D. Frankel, L. M. Goldman, R. L. McCrory, W. Seka, J. M. Soures, A. J. Burek, R. E. Deslattes, Opt. Commun. **38**, 196 (1981).

[3] D. W. Phillion and C. J. Hailey, Phys. Rev. A **34**, 4886 (1996).

[4] J. Workman and G. A. Kyrala, Rev. Sci. Instrum. **72**, 678 (2001).

[5] C. A. Back, J. Grun, C. Decker, L. J. Suter, J. Davis, O. L. Landen, R. Wallace, W. W. Hsing, J. M. Laming, U. Feldman, M. C. Miller, C. Wuest, Phys. Rev. Lett. **87**, 275003 (2001).

[6] K. B. Fournier, C. Constantin, C. A. Back, L. Suter, H. K. Chung, M. C. Miller, D. H. Froula, G. Gregori, S. H. Glenzer, E. L. Dewald, O. L. Landen, J. Quant. Spectrosc. Radiat. Transf. **99**, 168 (2006).

[7] K. B. Fournier, C. Constantin, J. Poco, M. C. Miller, C. A. Back, L. J. Suter, J. Satcher, J. Davis, and J. Grun, Phys. Rev. Lett. **92**, 165005 (2004).

[8] H. S. Park, D. M. Chambers, H. K. Chung, R. J. Clarke, R. Eagleton, E. Giraldez, T. Goldsack, R. Heathcote, N. Izumi, M. H. Key, J. A. Koch, J. A. Key, O. L. Landen, A. Nikroo, P. A. Patel, D. F. Price, B. A. Remington, H. F. Robey, R. A. Snavely, D. A. Steinman, R. B. Stephens, C. Stoeckl, M. Storm, M. Tabak, W Theobald, R. P. J. Town, J. E. Wickersham, B. B. Zhang, Phys. Plasmas **13**, 056309 (2006).

[9] R. Kauffman, in *Handbook of Plasma Physics*, edited by A. M. Rubenchik and S. Witlowsi (Elsevier Science, 1991), chap. 3, p. 111.

[10] H. Takabe, M. Yamanaka, K. Mima, C. Yamanaka, H. Azechi, N. Miyanaga, M. Nakatsuka, T. Jitsuno,

T. Norimatsu, and M. Takagi, Phys. Fluids **31**, 2884 (1988).

[11] J. Denavit and D. W. Phillion, Phys. Plasmas **1**, 1971 (1994).

[12] C. Constantin, C. A. Back, K. B. Fournier, G. Gregori, O. L. Landen, S. H. Glenzer, E. L. Dewald, and M. C. Miller, Phys. Plasmas **12**, 063104 (2005).

[13] F. Girard, J. P. Jadaud, M. Naudy, B. Villette, D. Babonneau, M. Primout, M. C. Miller, R. L. Kauffman, L. J. Suter, and D. J. Davis, Phys. Plasmas **12**, 092705 (2005).

[14] T. Okuno, S. Fujioka, H. Nishimura, Y. Tao, K. Nagai, Q. Gu, N. Ueda, T. Ando, K. Nishihara, T. Norimatsu, N. Miyanaga, Y. Izawa, K. Mima, A. Sunahara, H. Furukawa, A. Sasaki, Appl. Phys. Lett. **88**, 161501 (2006).

[15] D. Li and Y. Xia, Nano Lett. **3**, 555 (2003).

[16] C. Pan, Z.-Z. Gu, K. Nagai, Y. Shimada, K. Hashimoto, T. Birou, and T. Norimatsu, J. Appl. Phys. **100**, 016104 (2006).

[17] H. K. Chung, M. H. Chen, W. L. Morgan, Y. Ralchenko, and R. W. Lee, High Energy Density Physics **1**, 3 (2005).

[18] R. M. More, K. H. Warren, D. A. Young, and G. B. Zimmerman, Phys. Fluids **31**, 3059 (1988).

[19] N. Ohnishi, M. Nishikino, and A. Sasaki, J. Phys. IV France **133**, 1193 (2006).

FIGURE CAPTIONS

FIG.1. (Color online) Arrangement of the four x-ray diagnostics. The small block of nano-fiber-cotton material (0.8 mm thickness, 1.5 mm width, and 2.5 mm height) was attached to a 50-μm-thick polystyrene film. A slit was fielded at 1.5 mm in distance from the target surface to restrict the observation region.

FIG.2. (Color online) A Ti *K*-shell spectrum (solid line) measured by means of the x-ray streak spectrograph for the nano-fiber-cotton target at the time of highest electron temperature. Spectra calculated using the FLYCHK code were convoluted with the instrumental energy resolution. The synthetic spectra are calculated for 1.8 keV (dotted line), 2.3 keV (dashed line), and 2.8 keV (dash-dotted line) in electron temperature. An electron density of 8.8×10^{21} cm^{-3} is assumed. These spectra are normalized by the Lyα line intensity.

FIG.3. Two-dimensional x-ray images at different times for the planar Ti-foil (a)-(c) and for the titanium-dioxide nano-fiber-cotton target (d)-(f). The laser beams were incident from the left-hand side. The time origin was defined as 10% of x-ray emission peak measured by the the x-ray streak spectrograph. An intensity scale is mapped on the bottom.

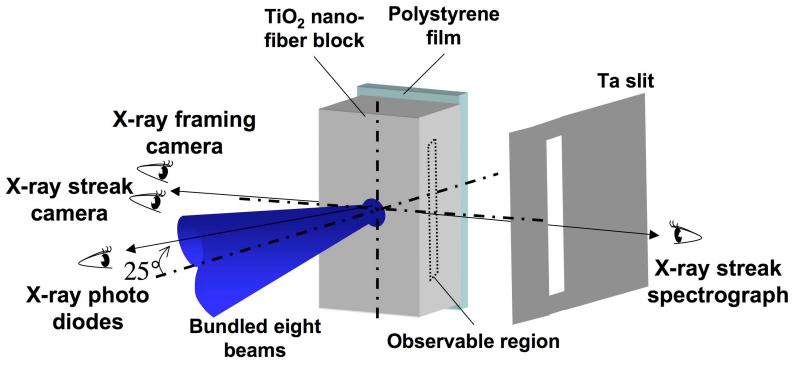

FIG. 1: M. Tanabe et al., Appl. Phys. Lett.

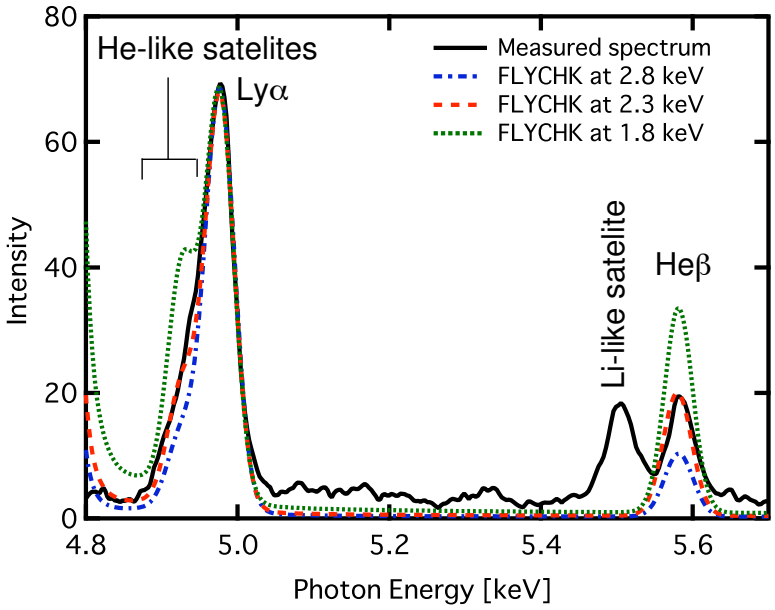

FIG. 2: M. Tanabe et al., Appl. Phys. Lett.

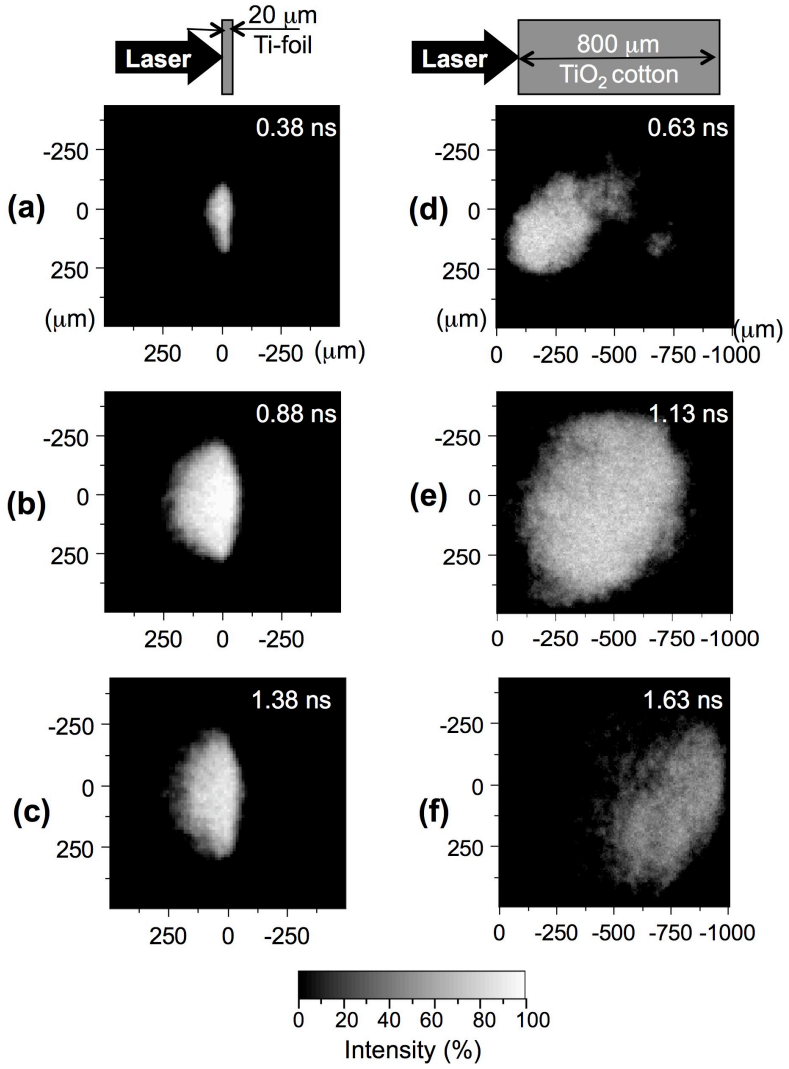

FIG. 3: M. Tanabe et al., Appl. Phys. Lett.